Cell Reports, Volume *28*

Supplemental Information

Spinal Neuropeptide Y1 Receptor-Expressing Neurons Form an Essential Excitatory Pathway for Mechanical Itch

David Acton, Xiangyu Ren, Stefania Di Costanzo, Antoine Dalet, Steeve Bourane, Ilaria Bertocchi, Carola Eva, and Martyn Goulding

Supplemental Information

Spinal NPY1R+ Neurons form an Essential Excitatory Pathway for Mechanical Itch

David Acton, Xiangyu Ren, Stefania Di Costanzo, Antoine Dalet, Steeve Bourane, Illarai Bertocchi, Carola Eva, and Martyn Goulding

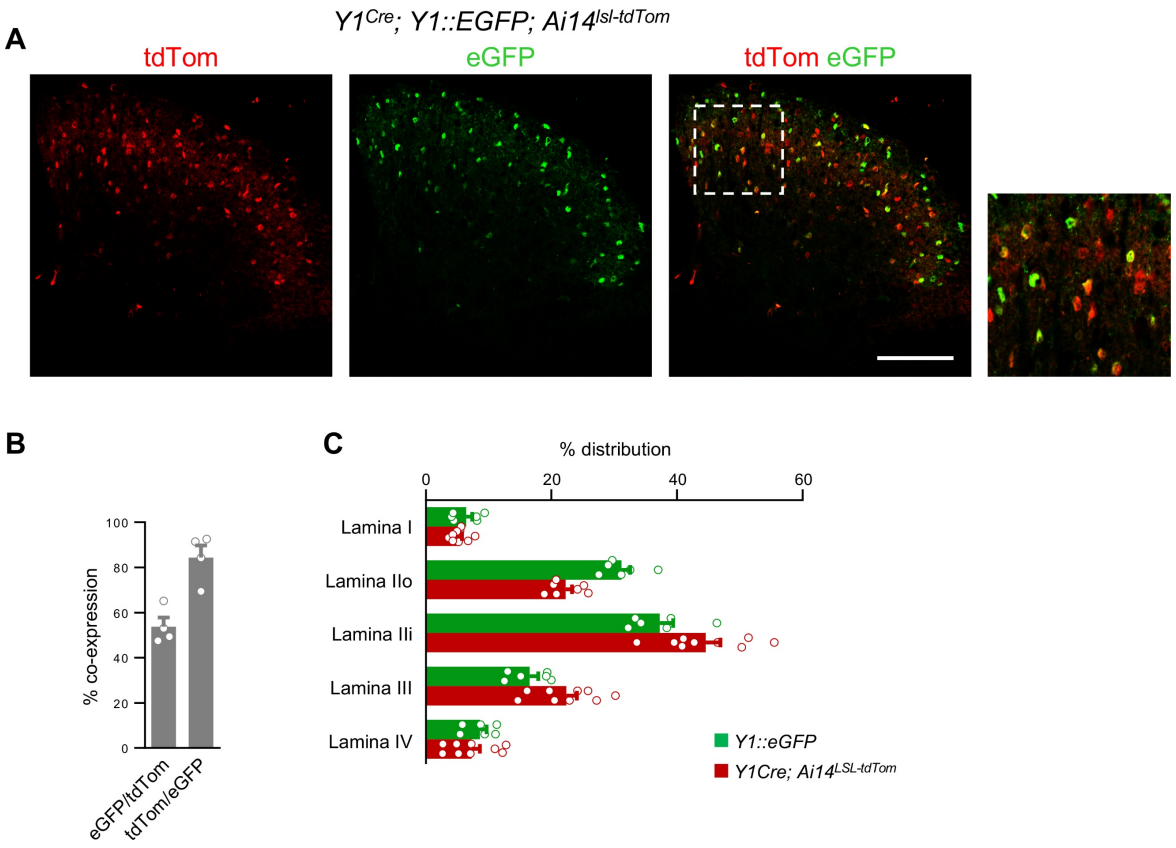

Figure S1 related to Figure 1. Characterization of *Y1::EGFP* expression.

(A) Sections from the lumbar spinal cord of a P42 *Y1^{Cre}; Y1::EGFP; Ai14$^{lsl\text{-}tdTom}$* mouse showing overlapping expression of tdTomato and eGFP. Scale bar: 100 µm. **(B)** Summary of tdTomato and eGFP co-expression (n = 4 mice). **(C)** Comparison of Y1-tdTomato and Y1-eGFP expression by lamina (n = 6-9 mice). Data: mean ± SEM.

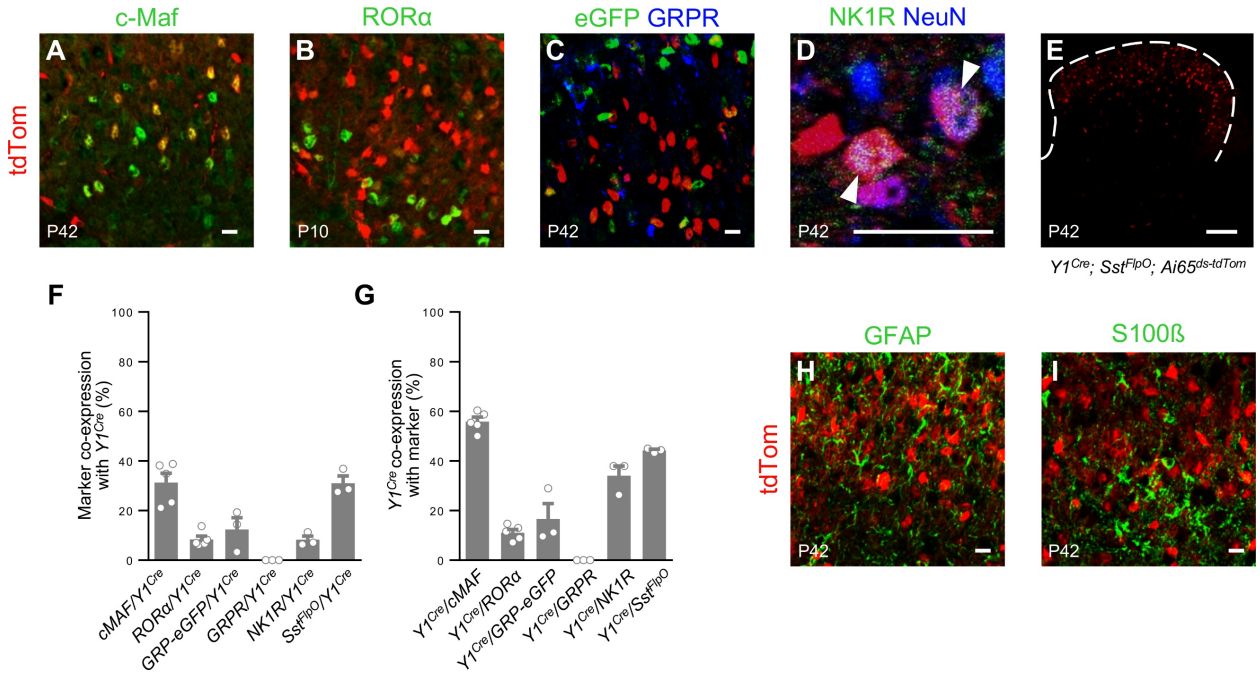

Figure S2 related to Figure 1. Co-expression of markers of dorsal horn cell populations with *Y1^{Cre}*.

(A-D) Sections of lumbar spinal cords showing co-expression of *Y1^{Cre}* with markers of dorsal horn excitatory neurons: cMaf co-expression was assessed by antibody staining in lumbar spinal cord sections from P42 *Y1^{Cre}; Ai14$^{lsl\text{-}tdTom}$* mice (A). RAR-related orphan receptor alpha (RORα) expression was assessed by antibody labelling in P10 *Y1^{Cre}; Ai14$^{lsl\text{-}tdTom}$* mice (B). Co-expression of *Y1^{Cre}* with gastrin releasing peptide (GRP) and antibody-labeled gastrin-releasing peptide receptor (GRPR) was assessed in P42 *Y1^{Cre}; Ai14$^{lsl\text{-}tdTom}$; GRP::eGFP* mice (C). Neurokinin-1 receptor (NK1R) co-expression was assessed by antibody staining in lumbar spinal cord sections from P42 *Y1^{Cre}; Ai14$^{lsl\text{-}tdTom}$* mice; an antibody against the pan-neuronal marker NeuN was employed to facilitate identification of Y1-tdTomato^{-} cells. Arrowheads: Y1-tdTomato^{-}/NK1R^{+} neurons (D). **(E)** Somatostatin (Sst) co-expression was assessed by comparing Y1^{+}/Sst^{+} neurons in P42 *Y1^{Cre}; Sst^{FlpO}; Ai65$^{ds\text{-}tdTom}$* mice. **(F and G)** Quantification of the data exemplified in panels A-E: the proportions of Y1^{Cre} neurons co-expressing markers of other neuronal populations (F) and of those other populations co-expressing tdTomato (G). **(H and I)** tdTomato did not colocalize with antibody-labeled GFAP (H) or S100ß (I), markers of glia. *n* = 3-5 mice for each condition. Scale bars: 100 µm. Data: mean ± SEM.

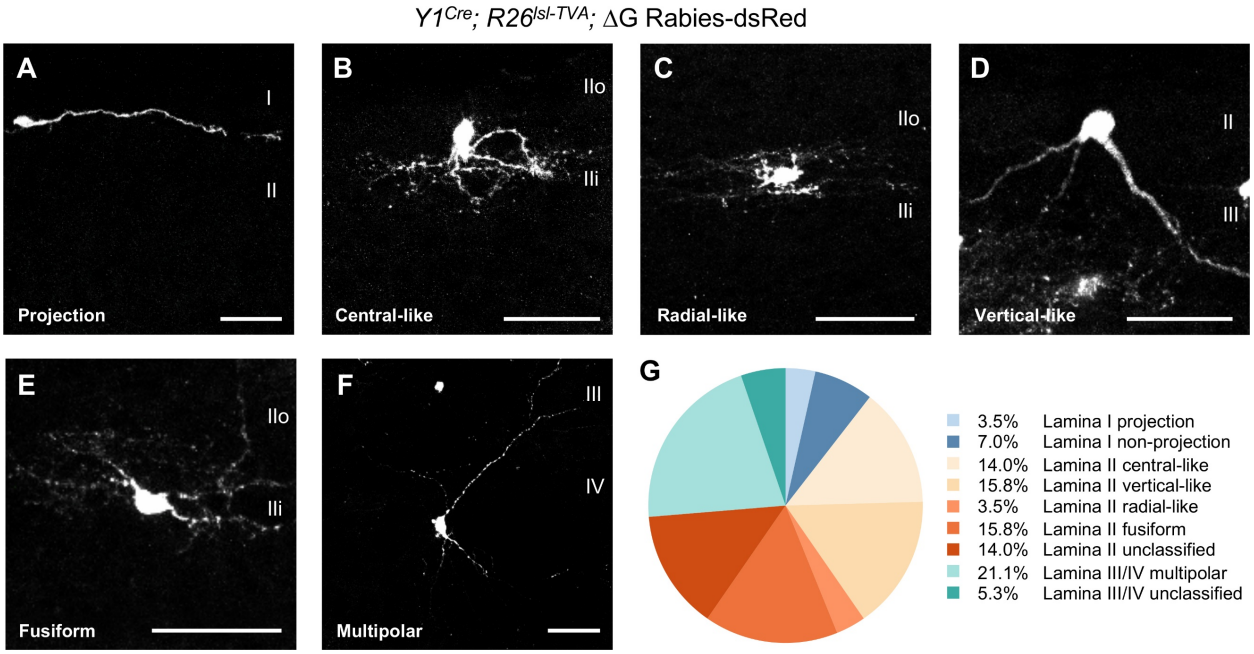

Figure S3 related to Figure 1. Morphological analysis of *Y1*^{Cre} neurons.

(A-F) Examples of laminae I-IV Y1^{Cre} neuron morphologies (red) in sagittal sections from the lumbar spinal cord of P15 *Y1*^{Cre}*; R26*$^{lsl\text{-}TVA}$ mice injected with EnvA ΔG dsRed-rabies virus at P10. **(G)** Quantification of Y1^{Cre} neuronal morphologies in laminae I-IV. n = 53 cells from 5 mice. Scale Bars: 50 µm.

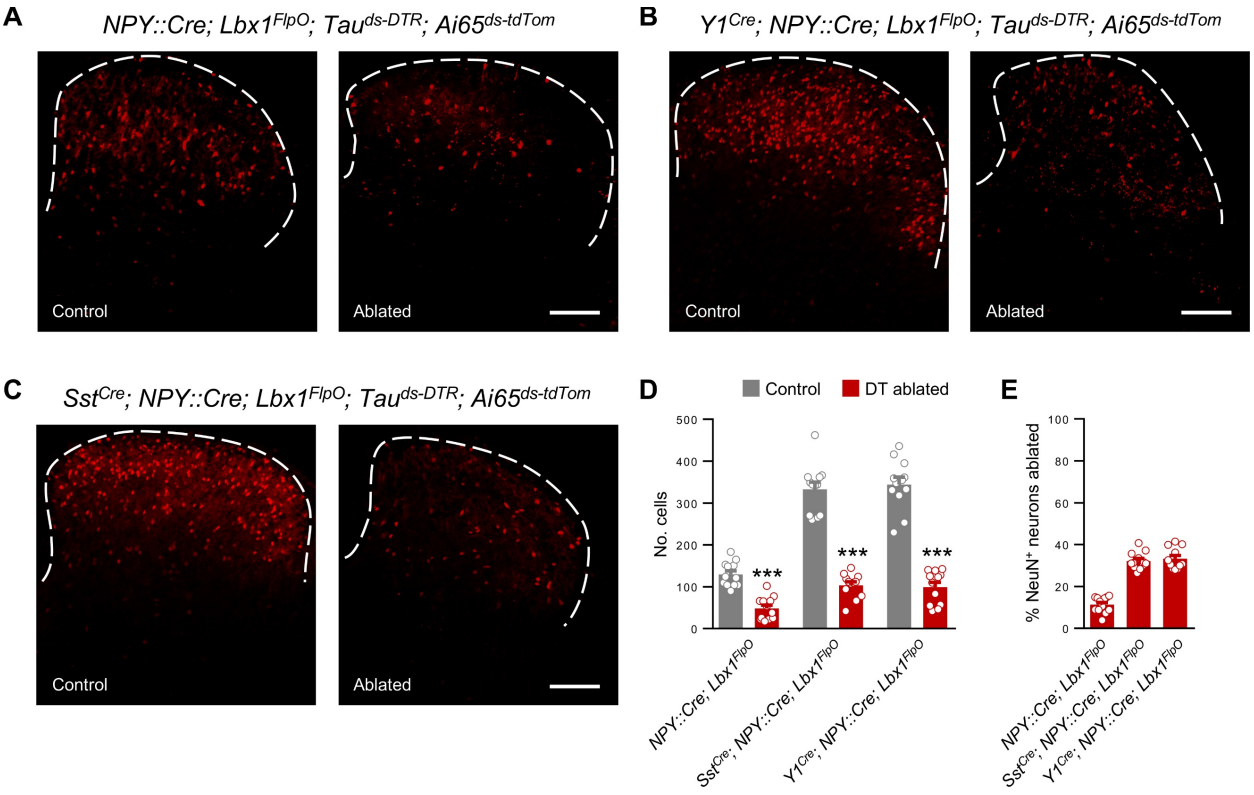

Figure S4 related to Figure 3. Ablation efficiency in NPY::Cre IN phenotype-recovery experiment.

(**A-C**) Transverse sections through the lumbar spinal cords of P49 mice treated with saline (control, left) or DT (ablated, right): *NPY::Cre; Lbx1^{FlpO}; Tau$^{ds\text{-}DTR}$; Ai65$^{ds\text{-}tdTom}$* (A), *Y1^{Cre}; NPY::Cre; Lbx1^{FlpO}; Tau$^{ds\text{-}DTR}$; Ai65$^{ds\text{-}tdTom}$* (B), *Sst^{Cre}; NPY::Cre; Lbx1^{FlpO}; Tau$^{ds\text{-}DTR}$; Ai65$^{ds\text{-}tdTom}$* (C). **(D)** Summary of cell numbers for each condition. The ablation efficiency, assessed as percentage reduction in cell number, did not differ between genotypes (one-way ANOVA, $p > 0.5$). **(E)** Percentage reduction of NeuN$^+$ neurons in laminae I-IV for each DT-treated phenotype. $n = 3$ sections from 4 mice per condition. Scale bars: 100 µm. ***$p < 0.001$. Data: mean ± SEM.

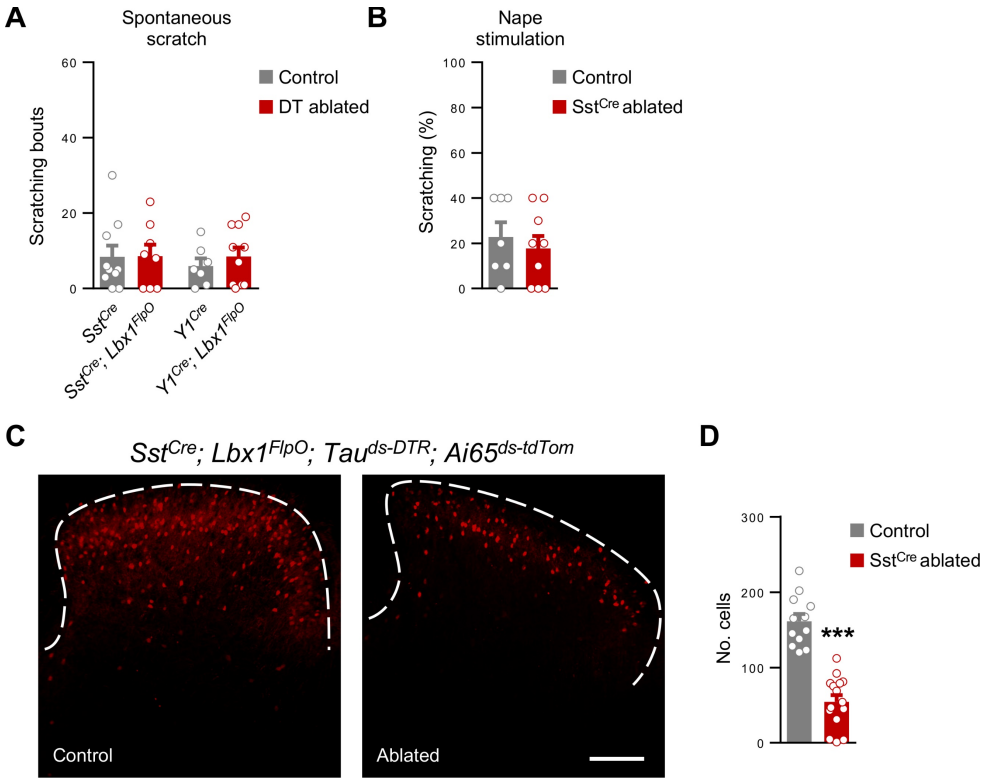

Figure S5 related to Figure 3. Sst^{Cre} neurons do not determine sensitivity to mechanical itch.

(A) Spontaneous scratching is unchanged in mice 1 week after ablation of dorsal horn Sst^{Cre} (*Sst^{Cre}; Lbx1^{FlpO}; Tau^{ds-DTR}; Ai65$^{ds-tdTom}$*; $n = 8$) or Y1^{Cre} neurons (*Y1^{Cre}; Lbx1^{FlpO}; Tau^{ds-DTR}; Ai65$^{ds-tdTom}$*, $n = 10$) compared with DT-treated controls lacking FlpO-dependent DT-receptor expression (*Sst^{Cre}; Tau^{ds-DTR}; Ai65$^{ds-tdTom}$*, $n = 10$; *Y1^{Cre}; Tau^{ds-DTR}; Ai65$^{ds-tdTom}$*, $n = 7$). **(B)** Scratching responses to stimulation of the nape by a 0.16 g von Frey hair are unchanged when Sst^{+} neurons are ablated in *Sst^{Cre}; Lbx1^{FlpO}; Tau^{ds-DTR}; Ai65$^{ds-tdTom}$* mice treated with DT ($n = 9$) compared with saline-treated controls ($n = 7$). **(C)** Sections of lumbar spinal cords from P49 *Sst^{Cre}; Lbx1^{FlpO}; Tau^{ds-DTR}; Ai65$^{ds-tdTom}$* mice treated with saline (control) or DT (ablated). **(D)** Summary of ablation efficiency (control, $n = 4$ mice; ablated, $n = 5$; 3 sections per cord). Scale bars: 100 µm. ***$p < 0.001$. Data: mean ± SEM.

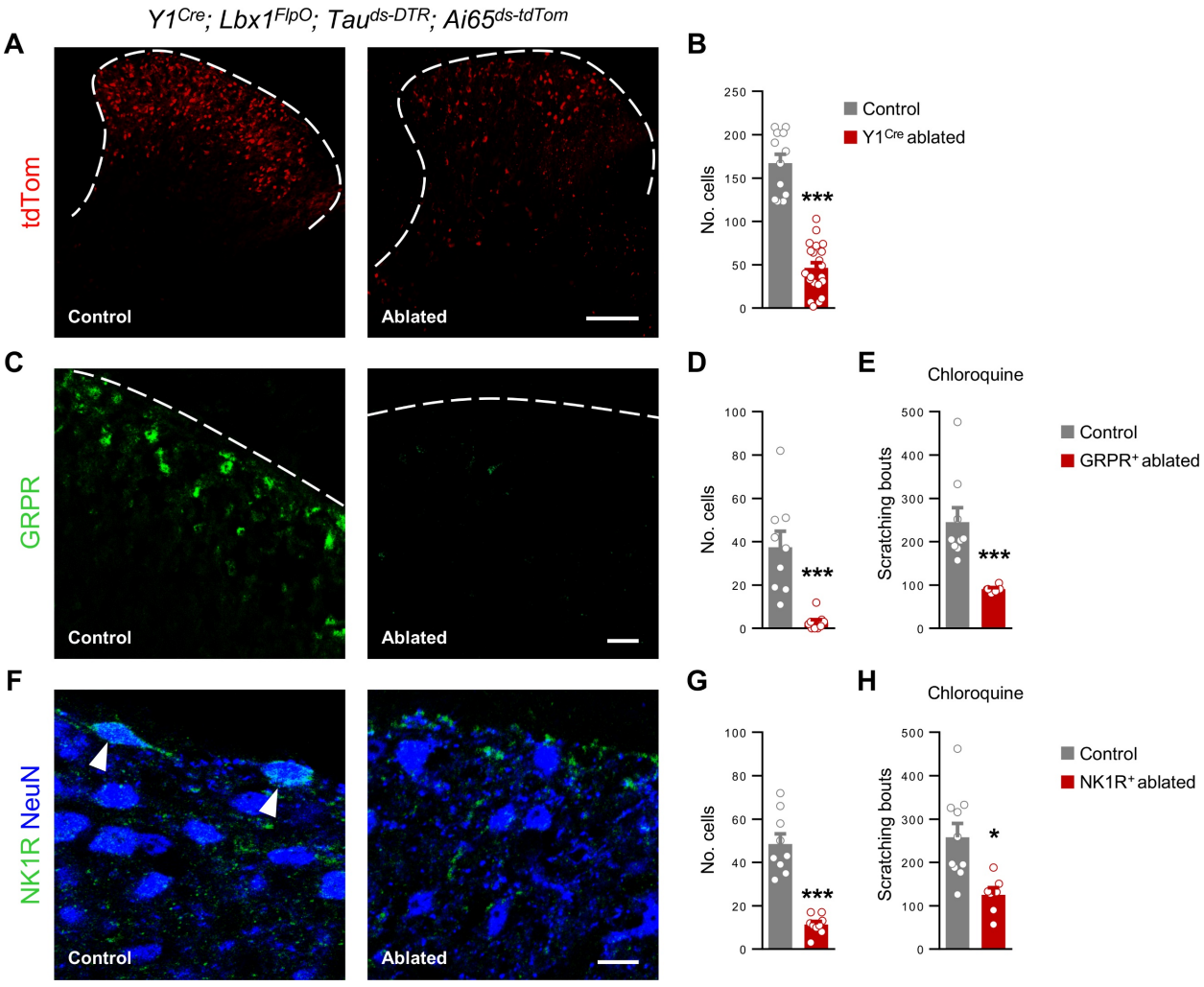

Figure S6 related to Figure 3. Efficiency of cell ablation.

(A) Sections of lumbar spinal cords from P49 *Y1^{Cre}; Lbx1^{FlpO}; Tau$^{ds\text{-}DTR}$; Ai65$^{ds\text{-}tdTom}$* mice treated with saline (control; left) or DT (ablated; right). Scale bar: 100 µm. **(B)** Summary of Y1^{Cre} neuron ablation efficiency (control, 6 cords; ablated, 7 cords; 3 sections per cord). (**C)** Sections from P42 wild type mice showing loss of GRPR immunoreactivity in the superficial dorsal horn at the cervical level 2 weeks after treatment with control SAP (left panel) or BOM-SAP (right panel) to ablate GRPR^{+} neurons. Scale bar: 20 µm. **(D)** Summary of GRPR^{+} neuron ablation efficiency (control, *n* = 3 mice; ablated, *n* = 3; 3 sections per cord). **(E)** Chloroquine-induced scratching is reduced in wild type mice 2 weeks following treatment with BOM-SAP (*n* = 6; controls, *n* = 8). **(F)** Sections from P42 wild type mice showing loss of NK1R immunoreactivity in the superficial dorsal horn at the cervical level 2

weeks after treatment with control SAP (left panel) or with SSP-SAP (right panel) to ablate $NK1R^+$ neurons. Scale bar: 10 µm. **(G)** Summary of $NK1R^+$ neuron ablation efficiency (control, $n = 3$ mice; ablated, $n = 3$; 3 sections per cord). **(H)** Chloroquine-induced scratching is reduced in wild type mice 2 weeks following treatment with SSP-SAP ($n = 7$; controls, $n = 10$). *$p < 0.05$, ***$p < 0.001$. Data: mean ± SEM.

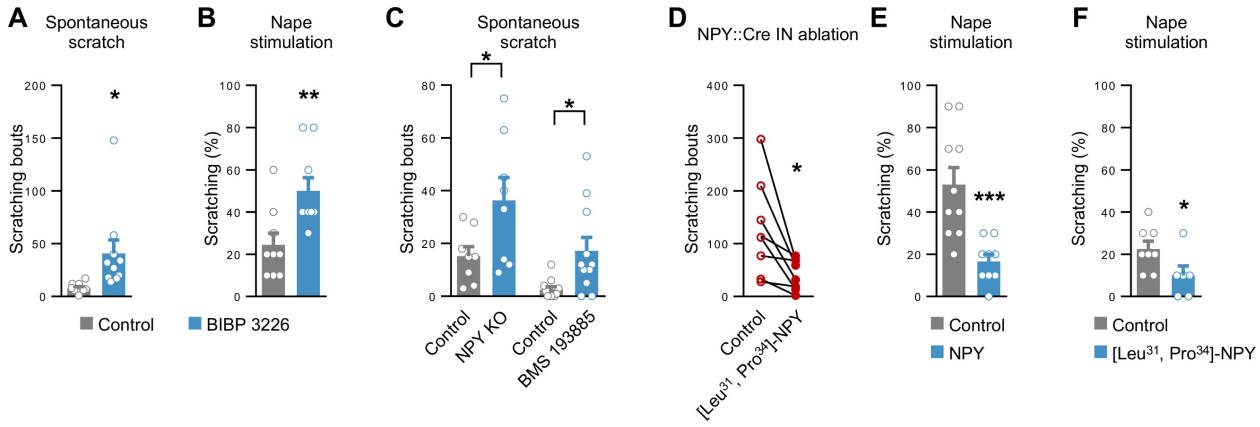

Figure S7 related to Figures 6 and 7. Y1 receptors modulate mechanical itch.

(A and B) I.t. injection of BIBP 3226 (5 µg in 10 µl) increases both spontaneous (A; $n = 10$; controls, $n = 10$) and evoked (B; $n = 9$; controls, $n = 9$) scratching. **(C)** Disruption of NPY-Y1 signaling increases spontaneous scratching in global NPY KO mice ($n = 8$; littermate control, $n = 8$), or following i.p. injection of wild type mice with the Y1 antagonist BMS 193885 (1 mg kg^{-1}, $n = 11$; vehicle, $n = 11$). **(D)** Spontaneous scratching in *NPY::Cre; Lbx1^{FlpO}; Tau$^{ds\text{-}DTR}$; Ai65$^{ds\text{-}tdTom}$* mice 1 week after DT treatment is reduced by i.t. injection of the selective Y1 agonist [Leu^{31}, Pro^{34}]-NPY (1.5 ng in 10 µl; $n = 8$) compared with vehicle. A two-tailed, paired t-test was used to assess statistical difference. **(E)** Evoked scratching is reduced when mice are injected with NPY (100 µg kg^{-1}, i.p., $n = 9$; vehicle, $n = 10$). **(F)** Scratching in response to nape stimulation is reduced following i.t. injection of [Leu^{31}, Pro^{34}]-NPY ($n = 6$; controls, $n = 8$). *$p < 0.05$, **$p < 0.01$, ***$p < 0.001$. Data: mean ± SEM.